

Supplementary Material

for the manuscript

Direct observation of pore collapse and tensile stress generation on pore wall due to salt crystallization

A.Naillon^{1,2,3}, P.Joseph², M.Prat^{1*}

¹*Institut de Mécanique des Fluides de Toulouse (IMFT), Université de Toulouse, CNRS, Toulouse, France*

²*LAAS-CNRS, Université de Toulouse, CNRS, Toulouse, France*

³*Univ Grenoble Alpes, CNRS, Grenoble INP, LRP, 38000 Grenoble, France*

A. Experimental set-up

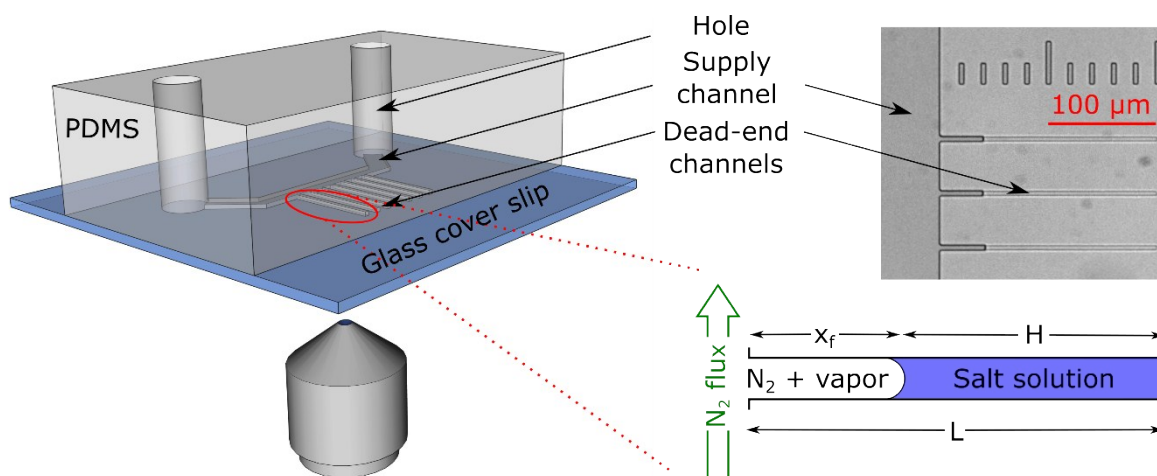


FIG. A1. (Color online) Schematic of the PDMS and glass microfluidic chip. Crystallization and wall deformations are observed in the dead-end channels.

The experimental set-up is composed of a large channel used for supplying the fluids: salt solution or gaseous nitrogen. 200 μm long smaller channels of $5 \times 5 \mu\text{m}^2$ square cross-section, referred to as pore channels, are positioned perpendicularly to the supply channel. Details on the microfluidic chip fabrication procedure are given in [11]. Note that estimates from the images suggest that the actual width is rather 4.5 μm . The latter value is adopted in what follows. The crystallization is triggered by evaporation of the sodium chloride solution confined in the pore channels. Salt solution is provided from the top hole through the supply channel and invades the pore channels. Once the device is filled, a dry N_2 flux is imposed from the bottom hole to empty the supply channel and isolates salt solution in the pore

* Corresponding author : mprat@imft.fr, +33 (0)5 34 32 28 83

channels. This flux is maintained during all the experiment. As a result of evaporation and pervaporation through the PDMS, the meniscus recedes into the pore channel, the ion mass fraction increases until the ion mass fraction C_{cr} marking the onset of crystallization is reached. This leads to the formation of a single crystal, most often within the liquid bulk away from the receding meniscus.

B. Hyperslow drying in PDMS channel (Fig.3 in main text)

The situation under consideration is sketched in Fig.B1.

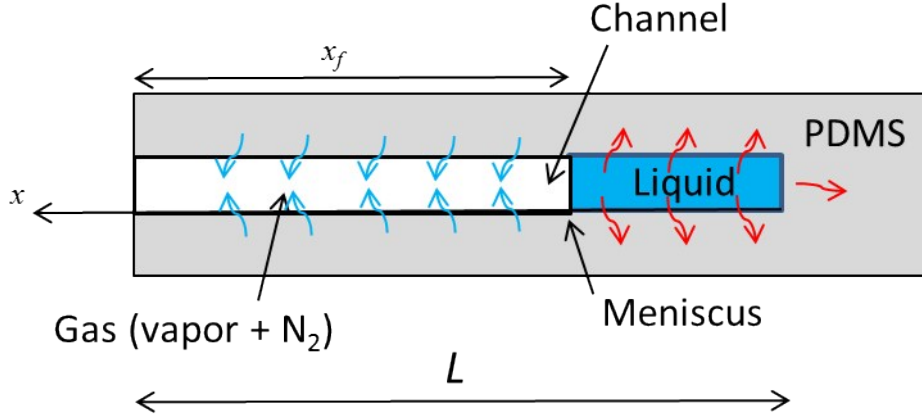


Fig.B1. Sketch of the considered situation. The blue arrows represent the water mass transfer from water saturated PDMS toward the section of the channel occupied by the gas phase. The red arrows represent the pervaporation process.

Let v_{pe} be the pervaporation velocity at the channel PDMS wall in the liquid plug. For simplicity, v_{pe} is assumed constant and uniform over the channel PDMS wall. Then a simple mass balance is expressed as

$$\rho W^2 \frac{dx_f}{dt} = \rho 3W(L - x_f)v_{pe} - J \quad (\text{B1})$$

where W is the channel width and the factor 3 comes from the fact that the channel has three PDMS wall (there is no pervaporation from the fourth one in glass). J is the “condensation” flux at the moving meniscus. The existence of J is explained as follows. If one considers that the vapor concentration at channel wall in the gaseous part of the channel (at least in the vicinity of the receding meniscus) is the equilibrium vapor concentration for pure water [20] (since the ions do not penetrate PDMS) and that the vapor concentration at the receding meniscus is less (the equilibrium vapor concentration of a NaCl saturated solution is 25% less than the equilibrium vapor concentration for pure water. When the solution is supersaturated, the vapor concentration at the meniscus can be even lower), then a water transfer must occur between the PDMS wall and the receding meniscus by diffusion in the gas phase. This “condensation” mechanism should contribute to slow down the meniscus. Considering J as a constant leads to a very good agreement with the experimental data.

Solving Eq.(B1) is straightforward. The solution reads

$$x_f = L - \left(\frac{J}{3\rho W v_{pe}} - \left(\frac{J}{3\rho W v_{pe}} - L \right) \exp\left(-\frac{3v_{pe}t}{W}\right) \right) \quad (\text{B2})$$

The pervaporation velocity is estimated in Appendix E ($v_{pe} = 2.3 \times 10^{-8}$ m/s). Using this value in Eq.(B2) with the dimension of the channel ($W \approx 4.5 \mu\text{m}$, $L = 200 \mu\text{m}$) and $J = 3.35 \cdot 10^{-14}$ kg/s leads to the very good agreement with the experimental data shown in Fig.3b (main text). However, it should be clear that the value of J has been adjusted to get this excellent agreement. A more comprehensive analysis would imply to predict J from the modelling of the coupled transport phenomena between the PDMS walls and the other regions (supply channel, pore channel, external air). This is left for a future study which will probably require some numerical simulations.

Also, as mentioned in the main text, the fact that the walls are humid (due to the presence of water in PDMS) in the gaseous part of the channel explains why the classical diffusion controlled evaporation in a tube (Stefan's tube situation) is negligible in the case of our experiment.

C. Meniscus acceleration induced by the crystal growth (Fig.2b in main text)

The situation analyzed in this sub-section is sketched in Fig.C1.

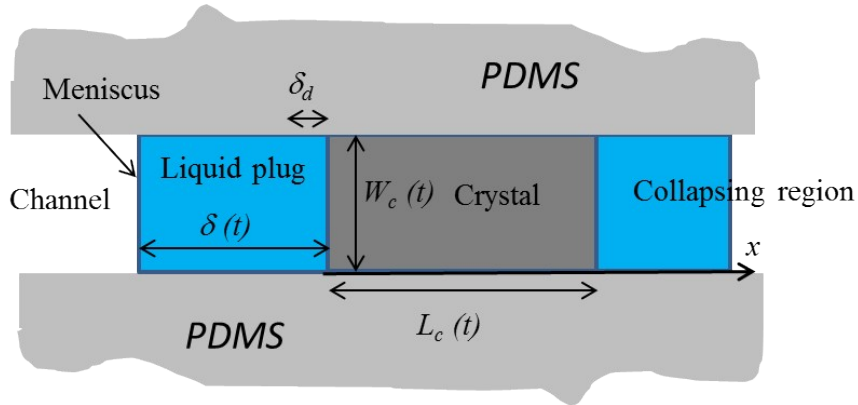


Fig.C1. Schematic of considered situation.

The objective is to explain the sudden acceleration of the meniscus during the crystal growth depicted in Fig.2b (strong increase in the slope of the curve showing the variation of the meniscus position as a function of time in Fig.2b). Referring to Fig.C1, The objective is thus to analyze the variation of the liquid plug length $\delta(t)$.

For convenience, the rapid variation of the crystal back face width $W_c(t)$ shown in Fig.2a is represented by a third degree polynomial,

$$W_c(t) = -8869.5 + 72.334 t - 0.19648 t^2 + 0.00017787 t^3 \quad \text{for } 348 \text{ s} \leq t \leq 364 \text{ s} \quad (\text{C1})$$

where t is the time in seconds and $W_c(t)$ is in μm .

The meniscus sudden acceleration is analyzed from the consideration of two effects, the channel expansion effect and the crystallization induced flow. The two effects are both taken into account to obtain the result shown in Fig.2b (inset). For simplicity, we begin with the consideration of each effect separately.

Channel expansion effect

This effect refers to the fact that the conservation of the liquid plug mass implies that the liquid plug length $\delta(t)$ must decrease in the channel when the width increases due to the growth of the crystal. The volume of the liquid plug on the left of the crystal in Fig.C1 is expressed as

$$V = \delta W_c^2 \quad (C2)$$

Since the duration of the meniscus acceleration period (~ 10 s) is small compared to the collapse period (~ 100 s), it is assumed that the mass loss due to pervaporation can be neglected. In other words, it is assumed that the volume V does not vary significantly. As a result,

$$\delta W_c^2 = \delta_0 W_{c0}^2 \quad (C3)$$

where the subscript « 0 » refers to values at the very beginning of the meniscus acceleration period. Thus,

$$\delta = \delta_0 \frac{W_{c0}^2}{W_c^2} \quad (C4)$$

Liquid flow induced by the crystallization

This effect refers to the fact that the crystal growth induced a flow directed on average toward the crystal in the adjacent liquid. As presented in [14], the kinematic condition at the crystal liquid interface reads

$$v_l \cdot \mathbf{n}_{cr} = \left(1 - \frac{\rho_{cr}}{\rho_l}\right) \mathbf{w}_{cr} \cdot \mathbf{n}_{cr} \quad (C5)$$

where \mathbf{w}_{cr} is the velocity of the crystal-solution interface, v_l is the liquid velocity at the crystal–liquid interface, \mathbf{n}_{cr} is the unit normal vector at the interface, ρ_{cr} is the crystal density (2160 kg/m³), ρ_l is the solution density (~ 1200 kg/m³). Based on the results shown in Fig.2, it is assumed that the crystal growth essentially occurs over the four faces of the crystal parallel to the channel wall during the very short period when the meniscus acceleration occurs (on the ground that the growth of the crystal faces perpendicular to the channel wall is quite weak during the considered period). Accordingly, the total flow rate induced in the liquid is estimated as

$$Q(t) \approx \left(\frac{\rho_{cr}}{\rho_l} - 1\right) 4 L_c W_c(t) \left(\frac{1}{2} \frac{dW_c(t)}{dt}\right) \quad (C6)$$

Then expressing that this flow rate should correspond to the meniscus displacement leads to

$$W_c^2 \frac{d\delta}{dt} = -Q(t) \approx -2 \left(\frac{\rho_{cr}}{\rho_l} - 1 \right) L_c W_c(t) \frac{dW_c(t)}{dt} \quad (C7)$$

Combining both effects

Both effects can be taken into account as follows. From Eq.(C2) and taking into account the flow rate induced by the salt precipitation yields,

$$\frac{dV}{dt} = \frac{d(\delta W_c^2)}{dt} = -Q(t) \quad (C8)$$

which can be expressed as

$$W_c^2 \frac{d\delta}{dt} + 2\delta W_c \frac{dW_c}{dt} = -Q(t) \quad (C9)$$

Then, taking into account Eq.(C6) leads to express Eq.(C9) as

$$W_c^2 \frac{d\delta}{dt} + 2\delta W_c \frac{dW_c}{dt} = -2 \left(\frac{\rho_{cr}}{\rho_l} - 1 \right) L_c W_c(t) \frac{dW_c(t)}{dt} \quad (C10)$$

or

$$W_c^2 \frac{d\delta}{dt} = - \left(2\delta W_c + 2 \left(\frac{\rho_{cr}}{\rho_l} - 1 \right) L_c W_c(t) \right) \frac{dW_c}{dt} \quad (C11)$$

Actually, the deformation of the channel occurs in the direction of the liquid plug over a distance which is smaller than the initial length δ_0 of the liquid plug. In other words, it is assumed that the channel deformation in the liquid plug region occurs over a distance δ_d from the crystal (with $\delta_d < \delta_0$).

Under these circumstances, the volume of the liquid plug can be expressed as,

$$V = (\delta - \delta_d) W_0^2 + \delta_d W_c^2 \quad \text{when } \delta \geq \delta_d \quad (C12)$$

$$V = \delta W_c^2 \quad \text{when } \delta \leq \delta_d \quad (C13)$$

Then the liquid plug mass conservation equation can be expressed as follows when $\delta \geq \delta_d$,

$$\frac{dV}{dt} = \frac{d((\delta - \delta_d) W_0^2 + \delta_d W_c^2)}{dt} = -Q(t) \quad (C14)$$

leading to

$$W_0^2 \frac{d\delta}{dt} + 2\delta_d W_c \frac{dW_c}{dt} = -Q(t) \quad (C15)$$

Substituting Eq.(C6) into Eq.(C15) leads to

$$W_0^2 \frac{d\delta}{dt} + 2\delta_d W_c \frac{dW_c}{dt} = -2 \left(\frac{\rho_{cr}}{\rho_l} - 1 \right) L_c W_c(t) \frac{dW_c(t)}{dt} \quad (C16)$$

$$W_0^2 \frac{d\delta}{dt} = - (2\delta_d W_c + 2 \left(\frac{\rho_{cr}}{\rho_l} - 1 \right) L_c W_c(t)) \frac{dW_c(t)}{dt} \quad (C17)$$

Eq.(C17) is used as long as $\delta \geq \delta_d$. When $\delta \leq \delta_d$, then one can use Eq.(C11). With $\delta_d = 2 \mu\text{m}$, which seems to be a reasonable value, using Eq.(C17) and Eq.(C11) together with Eq.(C1) leads to the results show in the inset of Fig.2b (where “model “ corresponds to the numerical values obtained from Eq.(C17) and Eq.(C11)).

D. Growth of crystal front face (Fig.4 in main text)

We consider the situation sketched in Fig.D1

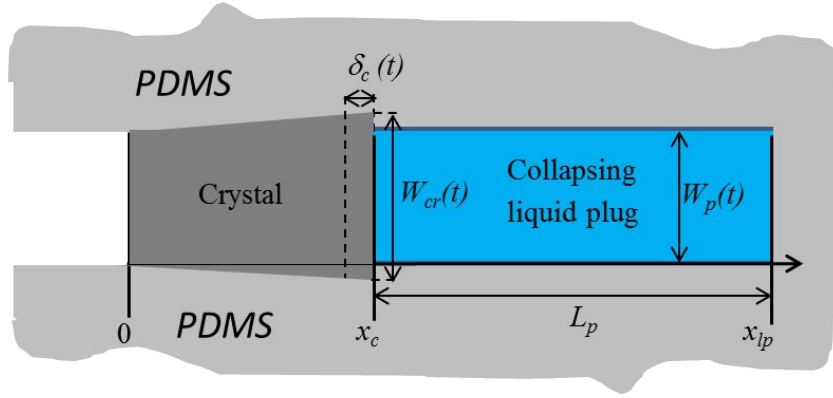


Fig.D1. Schematic of considered situation.

Let V be the volume of the collapsing liquid plug. Assuming that the ion mass fraction in the plug is very close to the equilibrium mass fraction C_{eq} on the ground that the NaCl precipitation reaction is quite fast, e.g. [14], the initial mass of salt in the plug is expressed as

$$m_0 = \rho_l C_{sat} V_0 \quad (D1)$$

where we have assumed that $C_{eq} \approx C_{sat}$ (C_{sat} is the solubility in the reference state). The mass of salt in solution at time t is

$$m = \rho_l C_{sat} V(t) \quad (D2)$$

where ρ_l is the solution density.

Then the mass flow rate of salt crystallizing is

$$\phi_s = \frac{dm}{dt} = \rho_l C_{sat} \frac{dV(t)}{dt} \quad (D3)$$

Denoting by W_{cr0} the size of the crystal when the collapse begins, Eq.(D3) can be expressed as

$$W_{cr0}^2 \rho_{cr} \frac{d\delta_c(t)}{dt} = -\rho_l C_{sat} \frac{dV(t)}{dt} \quad (D4)$$

where δ_c is the increase in the length of the crystal on the right (see Fig.D1) and ρ_{cr} is the crystal density. This yields

$$\frac{d\delta_c(t)}{dt} = -\frac{\rho_l C_{sat}}{W_{cr0}^2 \rho_{cr}} \frac{dV(t)}{dt} \quad (D5)$$

For simplicity we express $V(t)$ as $V(t) = W_p^2(t)L_p(t)$ where L_p is the length of the plug (L_p slightly varies owing to the crystal growth in the direction of channel dead end) and W_p is the width of the plug. Then Eq.(D5) can be expressed as

$$\frac{d\delta_c(t)}{dt} = -\frac{\rho_l C_{sat}}{W_{cr0}^2 \rho_{cr}} \frac{dW_p^2 L_p}{dt} \quad (D6)$$

This leads to

$$\frac{d\delta(t)}{dt} = -2W_p(t)L_p(t) \frac{\rho_l C_{sat}}{W_{cr0}^2 \rho_{cr}} \frac{dW_p(t)}{dt} - W_p^2(t) \frac{\rho_l C_{sat}}{W_{cr0}^2 \rho_{cr}} \frac{dL_p(t)}{dt} \quad (D7)$$

A fit of the experimental results for W_p shown in Fig. 2 (collapsing channel width) gives

$$W_p(t) = -15.46 + 0.14294t - 0.000224405t^2 \quad \text{for } 360 \text{ s} \leq t \leq 440 \text{ s} \quad (D8)$$

The plug is initially about 22 μm long. Thus $L_{p0} = 22 \mu\text{m}$ and

$$L_p(t) \approx L_{p0} - \delta_c(t) \quad (D9)$$

which leads to express Eq.(D7) as

$$\frac{d\delta_c(t)}{dt} = -2W_p(t)(L_{p0} - \delta_c(t)) \frac{\rho_l C_{sat}}{W_{cr0}^2 \rho_{cr}} \frac{dW_p(t)}{dt} + W_p^2(t) \frac{\rho_l C_{sat}}{W_{cr0}^2 \rho_{cr}} \frac{d\delta_c(t)}{dt} \quad (D10)$$

thus

$$\left(1 - W_p^2(t) \frac{\rho_l C_{sat}}{W_{cr0}^2 \rho_{cr}}\right) \frac{d\delta_c(t)}{dt} = -2W_p(t)(L_{p0} - \delta_c(t)) \frac{\rho_l C_{sat}}{W_{cr0}^2 \rho_{cr}} \frac{dW_p(t)}{dt} \quad (D11)$$

The collapsing channel cross section shape is expected to be somewhat different from a square shape since the glass cover plate does not deform and the deformation in the channel corner region should be less than in the middle of the channel walls. In other words, it can be argued that the cross section area of the collapsing channel is greater than W_p^2 . We introduce a shape factor F for taking into account this effect, $W_{peff} = F W_p$. This leads to express Eq.(D11) as,

$$\left(1 - 2F^2W_p^2(t) \frac{\rho_l C_{sat}}{W_{cr0}^2 \rho_{cr}}\right) \frac{d\delta_c(t)}{dt} = -2F^2W_p(t)(L_{p0} - \delta_c(t)) \frac{\rho_l C_{sat}}{W_{cr0}^2 \rho_{cr}} \frac{dW_p(t)}{dt} \quad (D12)$$

With $L_{p0} = 22 \mu\text{m}$, $\rho_l \approx 1200 \text{ kg/m}^3$, $\rho_{cr} = 2160 \text{ kg/m}^3$, $C_{sat} = 0.264$, $W_{ce0} \approx 6.2 \mu\text{m}$, solving numerically Eq.(D12) gives the results shown in Fig.4. As can be seen, a quite reasonable agreement is obtained with the experiment with $F = 1.22$.

E. Estimate of pervaporation velocity

We consider the situation sketched in Fig.D1.

The pervaporation velocity v_{pe} is defined as

$$v_{pe} = \frac{J_{pe}}{A_{pe}\rho_l} \quad (E1)$$

where ρ_l is the density of the solution, J_{pe} is the pervaporation rate and A_{pe} is the surface area of the PDMS walls limiting the collapsing region. Thus, v_{pe} is the velocity perpendicular to the wall induced in the solution by the pervaporation process.

The mass of solution in the collapsing region is expressed as

$$m_l = \rho_l W_p^2 L_p \quad (E2)$$

Where W_p is the width of the collapsing region and L_p is the length of the collapsing region (see Fig.D1).

The solution mass balance in the collapsing region is expressed as

$$\frac{dm_l}{dt} = J_{pe} + J_{cr} \quad (E3)$$

where J_{cr} is the mass flow rate resulting from the longitudinal growth of the crystal inside the collapsing region. The mass balance at the moving crystal front face reads [14],

$$J_{cr} = -\rho_{cr} w_{cr} W_{cr}^2 \quad (E4)$$

where w_{cr} is the velocity of the crystal front face, W_{cr} is the width of the crystal front face (see Fig.D1) and ρ_{cr} is the crystal density. Eq.(E4) can be expressed as

$$J_{cr} = \rho_{cr} W_{cr}^2 \frac{dL_p}{dt} \quad (E5)$$

Combining the above equations and noting that $A_{pe} = 3L_p W_p + W_p^2$, where the factor 3 comes from the fact that the pervaporation takes place only through three walls of the channel (no

pervaporation through the glass plate, see Fig.E1) and the factor W_p^2 corresponds to the surface of the channel tip, leads to the following expression of the pervaporation velocity:

$$v_{pe} = - \frac{\left[2L_p W_p \frac{dW_p}{dt} + \left(W_p^2 - \frac{\rho_{cr}}{\rho_l} W_{cr}^2 \right) \frac{dL_p}{dt} \right]}{3L_p W_p + W_p^2} \quad (\text{E6})$$

$\frac{dW_p}{dt}$ and $\frac{dL_p}{dt}$ are estimated from linear fits of the experimental data over the time period $362s \leq t \leq 392s$ corresponding to the initial period of collapse when the channel is not yet too deformed. This gives $\frac{dW_p}{dt} \approx -0.042 \mu\text{m/s}$ and $\frac{dL_p}{dt} \approx -0.037 \mu\text{m/s}$. With $L_p \approx 22 \mu\text{m}$, $W_p \approx 4.5 \mu\text{m}$, $W_{cr} = 6.5 \mu\text{m}$ (Fig.2a), $\rho_{cr} = 2160 \text{ kg/m}^3$, $\rho_l = 1200 \text{ kg/m}^3$, one obtains from Eq.(E6), $v_{pe} = 2.3 \times 10^{-8} \text{ m/s}$. This corresponds to a pervaporation flux $j_{pe} = \rho_l v_{pe} \approx 2.8 \times 10^{-5} \text{ kg/m}^2/\text{s}$. Interestingly, this estimate is consistent with the estimate that can be obtained from the formula used in [16]. This formula reads

$$j_{pe} = - \frac{\pi D_p \rho_{sat}}{W_p \ln \left(\frac{W_p}{4R} \right)} \quad (\text{E7})$$

where D_p ($D_p \approx 8 \times 10^{-10} \text{ m}^2/\text{s}$) is the diffusion coefficient for water in PDMS, ρ_{sat} is the saturation water concentration in PDMS ($\rho_{sat} = 0.72 \text{ kg/m}^3$). The geometry considered in [16] is the one of a very small channel in the middle of a hemi-cylindrical PDMS domain of radius R . With the approximation that R is about equal to the thickness of the PDMS layer (5 mm), using Eq.(E7) yields $j_{pe} = 4.4 \times 10^{-5} \text{ kg/m}^2/\text{s}$. This value is quite close to the one estimate above and thus is considered as a confirmation that the pervaporation process controls the collapse kinetics. The slightly lower value can be due to the activity of the solution which is less than pure water as well as the humidity in the external air which is not zero in our experiments.

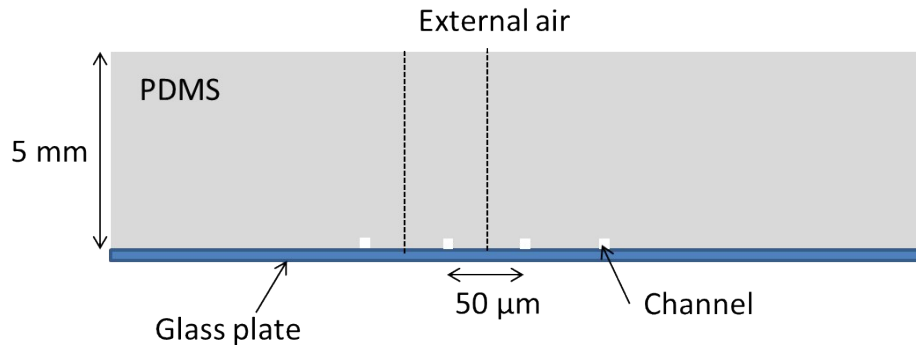


Fig. E1. Schematic of the experimental device cross-section.

F. Ion transport distribution in the thin film (Fig.6 in main text)

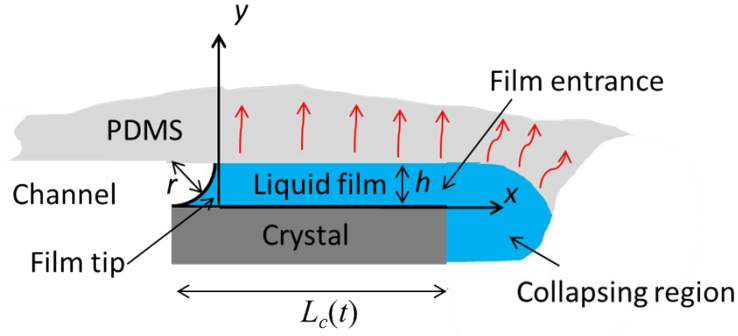


Fig.F1. Schematic of thin film confined between crystal and PDMS channel wall. The red arrows represent the pervaporation process. The figure is not at scale. The film thickness h is expected to be on the order of 10-100 nm whereas the crystal length $L_c \approx 10 \mu\text{m}$.

The 1d version of the ion transport equation in the film reads,

$$\frac{\partial C}{\partial t} + \frac{\partial}{\partial x}(vC) = D \frac{\partial^2 C}{\partial x^2} - a_v k_r (C - C_{eq}) \quad (\text{F1})$$

where C is the height-averaged ion mass fraction, v is the height averaged velocity, D is the diffusion coefficient of the ions in the solution, k_r is the precipitation reaction coefficient, a_v is

the specific surface area ($a_v = \frac{W_c}{W_c h} = h^{-1}$, where W_c is the width of the crystal), C_{eq} is the equilibrium ion mass fraction in the solution.

From mass conservation the height-averaged velocity in the solution is given by

$$v = -x \frac{v_{pe}}{h} \quad (\text{F2})$$

where v_{pe} is the pervaporation velocity ($v_{pe} = j/\rho_l$, where j is the pervaporation flux through the PDMS and ρ_l is the density of the solution). The maximum velocity (in absolute value) is at the entrance of the film (at $x = L_c$ in Fig.F1).

$$v_{max} = -v_{pe} \frac{L}{h} \quad (\text{F3})$$

Then, the Peclet number characterizing the competition between advective and diffusive transports along the film can be expressed as,

$$Pe = \frac{\|v_{max}\| L_c}{D} = \frac{v_{pe} L_c^2}{hD} \quad (\text{F4})$$

From the computation of pervaporation velocity ($v_{pe} = 2.3 \times 10^{-8}$ m/s, see SI Appendix E), one gets with $L_c \approx 10 \mu\text{m}$, $h \approx 10\text{-}100$ nm, $D = 1.3 \times 10^{-9}$ m²/s, $Pe \approx 0.03 - 0.3$. Based on the low

value of the Peclet number, a reasonable simplification is to neglect the convective term in Eq.(F1),

$$\frac{\partial C}{\partial t} = D \frac{\partial^2 C}{\partial x^2} - a_v k_r (C - C_{eq}) \quad (F5)$$

A characteristic time for diffusion is $\frac{L_c^2}{D} \approx 0.1$ s. This time is short compared to the crystal growth time (O(10-100s) as shown in Fig.2 in the main text). Thus, the evolution of the ion mass fraction in the film can be considered as quasi-steady.

$$D \frac{\partial^2 C}{\partial x^2} - a_v k_r (C - C_{eq}) = 0 \quad (F6)$$

Eq. (F6) is associated with the following boundary conditions,

$$D \frac{\partial C}{\partial x} = 0 \quad \text{at } x=0 \quad (F7)$$

$$C = C_{L_c} \quad \text{at } x=L_c(t) \quad (F8)$$

Eq.(F7) expresses that the ions cannot leave the film through the meniscus on the left whereas C_{L_c} (Eq.(F8)) is the ion mass fraction at the entrance of the film. The latter is estimated from Eq.(2) (main text) and the longitudinal growth rate of the front face. From Eq.(2) and Fig.2b,

$$w_{cr} = \frac{k_r \rho_l}{\rho_{cr}} (C_{L_c} - C_{eq}) = \frac{\Delta W}{\Delta t} \approx \frac{180.04 - 177.69}{402 - 348} = 4.35 \times 10^{-2} \mu\text{m/s} \quad . \text{ With } \rho_{cr} = 2160 \text{ kg/m}^3, \rho_l = 1200$$

kg/m³, and $k_r \sim 2.3 \cdot 10^{-2}$ m/s [14], one obtains $C_{L_c} - C_{eq} = 0.000034$.

$C^* = C - C_{eq}$. Eqs. (F6-F7) are expressed as

$$D \frac{\partial^2 C^*}{\partial x^2} - a_v k_r C^* = 0 \quad (F9)$$

$$D \frac{\partial C^*}{\partial x} = 0 \quad \text{at } x=0 \quad (F10)$$

$$C^* = C_{L_c} - C_{eq} \quad \text{at } x=L_c(t) \quad (F11)$$

The solution of Eq.(F9) reads

$$C^* = C_1 \exp(\lambda x) + C_2 \exp(-\lambda x) \quad (F12)$$

where $\lambda = \sqrt{\frac{a_v k_r}{D}}$. After substitution in Eqs.(F10) and (F11), constants C_1 and C_2 are determined. the solution reads,

$$C^* = (C_{L_c} - C_{eq}) \frac{(\exp(\lambda x) + \exp(-\lambda x))}{(\exp(\lambda L_c) - \exp(-\lambda L_c))} \quad (F13)$$

or

$$C = C_{eq} + (C_{L_c} - C_{eq}) \frac{(\exp(\lambda x) + \exp(-\lambda x))}{(\exp(\lambda L_c) - \exp(-\lambda L_c))} \quad (\text{F14})$$

The length scale $1/\lambda$ is on the order of 100 nm, thus much smaller than the length of the crystal ($\sim 10 \mu\text{m}$). As a result, the ion mass fraction is greater than C_{eq} only over a small region at the entrance of the film (on the right). This is illustrated in Fig.6 in the main text where ion mass fraction profiles along the film given by Eq.(F14) are plotted.

It can be argued that we have considered that the value of the diffusion coefficient in the thin film was the same as in a non-confined liquid. Actually, discussions with experts and a short look at literature indicate that the confinement must be much more severe ($h \sim 1 \text{ nm}$) for expecting a noticeable impact of confinement of ion diffusion properties in the film.

G. Estimate of collapsing pressure

Collapsing pressure is estimated from simulations performed with Comsol Multiphysics 5.2©, a commercial software based on the finite element method. Because of the elongated geometry of the channel, we assume that the problem can be simplified as a plane stress problem. Thus, the simulations are performed in 2 dimensions. Moreover, the deformation of PDMS and glass are assumed to be linearly elastic. The mechanical model is based on Hooke's law applied to both materials, i.e. glass and PDMS:

$$\sigma = \frac{E}{1 + \nu} \left(\varepsilon + \frac{\nu}{1 - 2\nu} \text{Tr}(\varepsilon) \mathbf{I} \right), \quad (\text{G1})$$

where σ , ε and \mathbf{I} , are the stress tensor, the strain tensor and the identity tensor, respectively. E (MPa) and ν are the young modulus of the considered material and its Poisson coefficient with $E_{PDMS}=1.2 \text{ MPa}$, $E_{glass}=64 \text{ GPa}$, $\nu_{PDMS}=0.45$ and $\nu_{glass}=0.45$.

On channel walls, a pressure load is imposed as boundary condition:

$$\sigma \cdot \mathbf{n} = -P_s \cdot \mathbf{n}, \quad (\text{G2})$$

where \mathbf{n} is the wall normal unit vector.

Fig.G1 shows results for a homogeneous normal stress of 0.3 MPa. Computation is not performed for higher (negative) pressure because the mesh distorted too much to be stable. From the results obtained in the range of normal stress $[0, 0.3 \text{ MPa}]$, it is inferred that a value of 0.5-0.6 MPa is a good order of magnitude of the pressure needed to collapse the channel in the middle of the collapsing region.

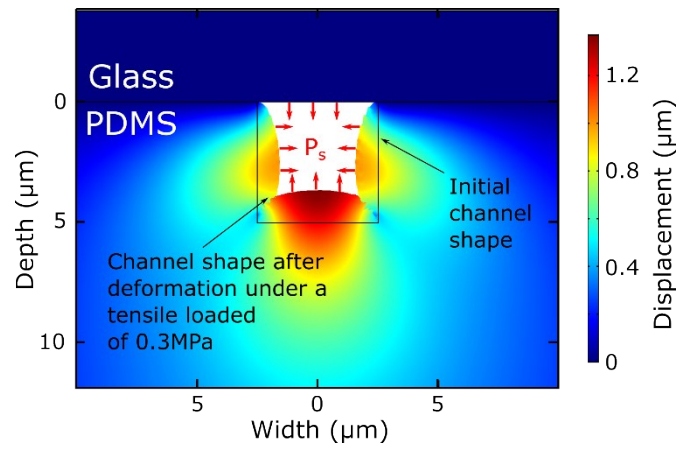


Fig. G1. Computation of the pore channel deformation under a homogeneous mechanical tensile load of 0.3MPa.